Cryobiology 78 (2017) 115–118

Contents lists available at ScienceDirect

Cryobiology

journal homepage: www.elsevier.com/locate/ycryo

Thermal thresholds of cardiovascular HL-1 cell destruction by cryothermal exposure

Jeunghwan Choi [a, b], John Bischof [a, c, d, *]

[a] Department of Mechanical Engineering, University of Minnesota, Minneapolis, MN, USA
[b] Department of Engineering, East Carolina University, Greenville, NC, USA
[c] Institute for Engineering in Medicine, University of Minnesota, Minneapolis, MN, USA
[d] Department of Biomedical Engineering, University of Minnesota, Minneapolis, MN, USA

ARTICLE INFO

Article history:
Received 16 February 2017
Received in revised form
16 June 2017
Accepted 17 June 2017
Available online 20 June 2017

Keywords:
Cryosurgery
Cryotherapy
HL-1 cardiomyocytes
Atrial fibrillation
Biophysics
Intracellular ice formation
Dehydration

ABSTRACT

The use of thermal based therapies for treatment of atrial fibrillation is increasing. While numerous reports are available in the literature regarding the efficacy of cryotherapy on pulmonary vein survival, there are no reports specifically at the cellular level that establish thermal thresholds and mechanisms of cellular destruction. The current article reports on the response of HL-1 cardiomyocytes to cooling rates and end temperatures during cryothermal exposure. The focus is on establishment of in vitro thresholds while also establishing mechanisms of action due to biophysical events (i.e. intracellular ice formation and water transport).

HL-1s, a murine cardiac muscle cell line with differentiated cardiac morphological, biochemical, and electrophysiological properties, were cultured as described in Ref. [4]. Briefly, the cells were allowed to proliferate in 75 cm^2 tissue culture flasks coated with gelatin/fibronectin. The cells were grown in a 5% CO_2, 37 °C incubator with Claycomb media further supplemented with 10% Fetal Bovine Serum, Noreprinephrine, L-Ascorbic Acid, and L-Glutamine (SAFC Biosciences, Lenexa, KS). The cultured cells were trypsinized (0.05% trypsin, Life Technologies, NY) and harvested as suspensions for experiments. Trypsin was inactivated using equal parts soybean trypsin inhibitor solution (2.35×10^{19} M). Following centrifugation at 500*g* for 5 min, supernatant was aspirated from cell pellet and cells were re-suspended to a final cell concentration of $5–6 \times 10^5$ cells/ml.

Freeze-thaw experiments using a cryomicroscope were performed as described in Ref. [3]. Briefly, 5–10 ml of cell suspensions were placed in a circular quartz crucible, mounted on a cryostage (BCS 196, Linkam, Surrey, UK), and imaged with a light microscope (BX50, Olympus, Japan). In order to avoid supercooling (non-equilibrium freezing) samples were preconditioned (prenucleated) by setting the temperature as −2 °C and by tapping the edge of the sample cover slip with a liquid nitrogen-chilled tip. This brought about nucleation and crystal growth. The samples were quickly heated to avoid excessive crystal growth, but the temperature was kept below the liquidus temperature (within 0.5 °C) to bring about a state where a small amount of ice nuclei would remain. This prenucleation step assured that the subsequent cooling would result in immediate (equilibrium condition) freezing (crystal growth). The cooling rate after prenucleation was varied between 0.5 and 130 °C/min and samples reached a low-end temperature between −5 and −60 °C. They were held at the end temperatures for 0–5 min, then rapidly thawed back to room temperature at 130 °C/min.

A membrane dye exclusion assay was used in this study for a simple comparative analysis of viability. Viability was assessed

* Corresponding author. Department of Mechanical Engineering, University of Minnesota, 111 Church St. SE, Minneapolis, MN 55455, USA.
E-mail address: bischof@umn.edu (J. Bischof).

http://dx.doi.org/10.1016/j.cryobiol.2017.06.007
0011-2240/

15 min post-thaw using 10 μM Hoechst 33342 (Sigma-Aldrich, MO) and 5 μg/ml propidium iodide (PI). Multiple fields amounting to at least 100 cells were counted using fluorescence.

A biophysical model of cellular freezing [5,6] was applied to the cryo experiment results to determine the cell-type dependent membrane water permeability and propensity to form intracellular ice. The model describes the change in cellular volume from a transport of intracellular water due to osmotic balancing effects during freezing to be:

$$\frac{dV}{dT} = \frac{L_p A}{B}(\Delta\pi) \tag{1}$$

where V is the cell volume (μm^3); T is the temperature (K); T_{ref} is the reference temperature (273.15 K); A is the cell surface area (μm^2); R is the gas constant (8.314 J/mol K); B is the cooling rate (degC/min); and $\Delta\pi$ is the osmotic pressure difference across the cell membrane. The cell membrane permeability (L_p) is defined using an Arrhenius relationship:

$$L_p = L_{pg} \exp\left[-\frac{E_{Lp}}{R}\left(\frac{1}{T} - \frac{1}{T_{ref}}\right)\right] \tag{2}$$

where L_{pg} is the membrane hydraulic permeability at T_{ref} (μm/min atm) and E_{Lp} is the activation energy for water transport (kcal/mol). The volume, V and area, A were determined from cryomicroscopy images recorded during freezing by correlating an effective diameter associated with the scaled/measured cross sectional area of the cell in planar focus with an assumed sphere for the cell.

The intracellular ice formation (IIF) model used in this study [10] is based on the assumption that the probability of IIF (PIF) can be associated with surfaced catalyzed nucleation (SCN) and that volume catalyzed nucleation (VCN) and intercellular nucleation pathway effects [1] are negligible:

$$PIF^{SCN} = 1 - \exp\left(-\frac{1}{B}\int_{T_{seed}}^{T} AI^{SCN} dT\right) \tag{3}$$

Here, T_{seed} is the ice seeding temperature (K) and I^{SCN} is the crystal nucleation frequency:

$$I^{SCN} = \Omega^{SCN} \exp\left(-\frac{\kappa^{SCN}}{\left(T - T_f\right)^2 T^3}\right) \tag{4}$$

where Ω is the kinetic heterogeneous nucleation parameter ($m^{-2}s^{-1}$), κ is the thermodynamic heterogeneous nucleation parameter (K^5), and T_f is the equilibrium freezing temperature of the intracellular fluid. The IIF parameters Ω and κ were determined for a range of fast cooling rates (50–130 °C/min) by analyzing the recorded images of cells during fast cooling. The PIF for each cell type was assumed to correspond to the ratio of cells which have darkened versus the total number of cells at a given temperature. The darkening, a sudden opaque flashing of the cell, was assumed to indicate the formation of large amounts of ice within the cell. Data from the cooling responses of 200 + cells were pooled in determining IIF kinetics.

Fig. 1a and b shows the post-thaw viability results for cells which underwent freezing under varied cooling rates and end temperatures, respectively. A peak survival rate of 5 °C/min was observed across all cell types with survival falling for faster or slower rates (Fig. 1a). The "inverted U" survival curve thus formed was qualitatively similar to those observed previously in other cell types [7]. It can be seen that a lower end temperature corresponds to lower survival [Fig. 1b] and even under a cooling rate advantageous for survival (i.e. 5 °C/min) the survival was below 10% at −60 °C.

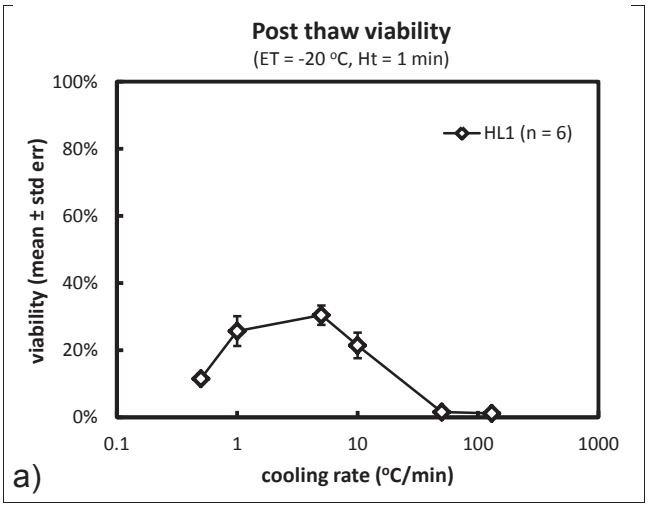

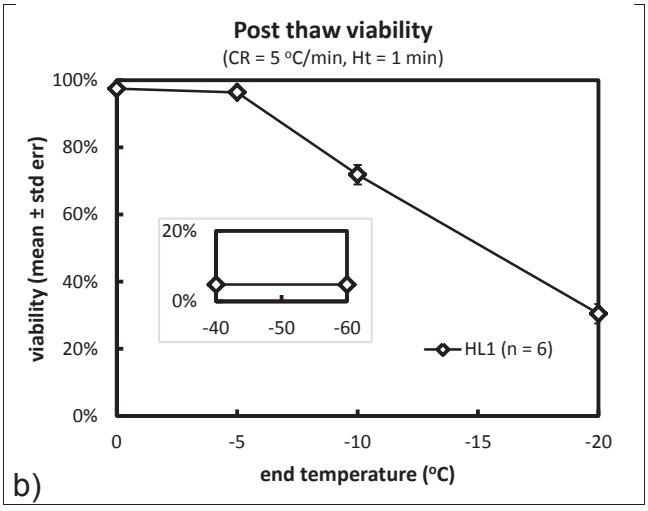

Fig. 1. (a). Post-thaw viability results for HL-1 cell suspensions which underwent freezing. Cells were cooled at varied rates to an end temperature of −20 °C and held for 1 min prior to thawing at 130 °C/min. Viability was determined using a membrane dye (Hoechst & Propidium Iodide) exclusion assay. (**b**). Post-thaw viability results for HL-1 cell suspensions which underwent freezing. Cells were cooled at 5 °C/min to varied end temperatures and held for 1 min prior to thawing at 130 °C/min.

Videographs depicting change in cellular volume during slow cooling and cumulative intracellular ice formation during fast cooling are shown in Fig. 2 and are graphically summarized in Figs. 3 and 4, respectively. The dynamic response at 10 °C/min appears to show the initial delay in volume change at a relatively faster cooling rate compared with 5 °C/min while the final change in volume is similar at lower temperatures (Fig. 3). Cumulative IIF results show the rise in total IIF observed with faster cooling rates (Fig. 4), while the onset and initial rise in cumulative IIF displayed a shift based on cooling rate, similar to results observed previously by others [11]. The biophysical parameters based on applying the